

X-RAY SPECTRUM OF THE HIGH POLARIZATION QUASAR PKS 1510-089

K. P. Singh ^{1,4}, C. R. Shrader ^{2,3,5}, and I. M. George ^{2,3,6}

Received _____; accepted _____

To appear in *The Astrophysical Journal*, 1997 December 1

arXiv:astro-ph/9708073v1 8 Aug 1997

¹X-ray Astronomy Group, Tata Institute of Fundamental Research, Mumbai 400 005, India

²Laboratory for High Energy Astrophysics, NASA/GSFC, Greenbelt, MD 20771

³Also Universities Space Research Association, 7501 Forbes Blvd, Seabrook MD 20706

⁴singh@tifrvax.tifr.res.in

⁵shrader@grossc.gsfc.nasa.gov

⁶ian.george@gsfc.nasa.gov

ABSTRACT

We present results on the X-ray spectra of the radio-loud, high-polarization quasar, PKS 1510-089, based on new data obtained using *ASCA*, and from archival *ROSAT* data. We find the X-ray spectrum obtained by *ASCA* to be unusually hard, with the photon index, $\Gamma=1.30\pm 0.06$, while the (non-simultaneous) *ROSAT* data indicate a steeper spectrum with $\Gamma=1.9\pm 0.3$. However, we find the X-ray flux at 1 keV to be within $\sim 10\%$ during both observations. Thus we suggest the most likely explanation is that there is a break (with $\Delta\Gamma \geq 0.6$) in the underlying continuum at ~ 0.7 keV.

Although the sample of high-polarization quasars for which high quality X-ray spectra are available is small, flat X-ray spectra seem to be the characteristic of these objects, and they also appear to be harder than that of the other radio-loud but low-polarization quasars. The multiwavelength spectrum of PKS 1510-089 is similar to many other γ -ray blazars, suggesting the emission is dominated by that from a relativistic jet. A big blue-bump is also seen in its multiwavelength spectrum, suggesting the presence of a strong thermal component as well.

Subject headings: galaxies:active – galaxies:nuclei – polarization – quasars: individual (PKS 1510-089) – radiation mechanism:non-thermal – X-rays: galaxies

1. INTRODUCTION

High polarization quasars (HPQs), along with BL Lac objects, form a subset of active galactic nuclei (AGN) known as blazars. HPQs are among the most energetic AGN. They are characterized by strong and variable radio, infrared and optical continuum emission with a high degree of polarization. Blazars are also strong and variable soft X-ray emitters (Brunner et al. 1994), and recently have also been found to emit ≥ 100 MeV γ -rays (Thompson et al. 1993). The X-ray spectral measurements of blazars have shown that the HPQs tend to have flatter spectral indices than the BL Lac objects (Sambruna et al. 1994). The uncertainties in these measurements of spectral indices are, however, generally large due to the small bandwidth, poor sensitivity, and low-energy absorption in the interstellar medium. There is also a general dearth of broad-band spectral measurements of HPQs extending to hard X-rays, the few exceptions being 3C 279 and 3C 345 (Makino 1989), PKS 1510-089 (Singh, Rao, & Vahia 1990), PKS 0537-441 (Sambruna et al. 1994), 3C 390.3 (Eraclous, Halpern, & Livio 1996), and a serendipitous detection of PKS 1502+106 (George et al. 1994). We chose to carry out X-ray spectral measurements of PKS 1510-089 with the *ASCA* observatory as previous measurements with the *EXOSAT* Observatory, reported by Singh et al. (1990) and Sambruna et al. (1994), indicated an unusually flat X-ray spectrum.

Radio source PKS 1510-089 was first identified optically as a quasar with an ultraviolet excess, a visual magnitude of 16.5 (Bolton & Ekers 1966), and a redshift of $z = 0.361$ measured from its emission line spectrum (Burbidge & Kinman 1966). Optical polarimetric observations by Appenzeller & Hiltner (1967) detected strong ($10.9\% \pm 3.8\%$) polarization at a position angle of $177^\circ \pm 9^\circ$. The strong variability of its optical brightness was first reported by Lu (1972) who monitored it for 5 years. Subsequently it was found that its B magnitude had varied by ~ 6 magnitudes since 1899.6 (Liller & Liller 1975). *The range of brightness spanned is larger than that known for any other quasar.* Its radio emission

exhibits very rapid, large amplitude variations in both total and polarized flux (Aller, Aller & Hodge 1981; Aller, Aller & Hughes 1996). It is a core dominated radio source with a *one-sided* jet which subtends about $8''$ in the 20-cm waveband (O’Dea, Barvainis & Challis 1988). Strong infrared (see Landau et al.1986), millimeter (see Steppe et al.1988), and UV emission (Malkan & Moore 1986) have also been detected from PKS 1510-089. γ -ray emission from PKS 1510-089 has also been detected by the *EGRET* instrument on *CGRO* (Thompson et al 1993, Sreekumar et al.1996) with a flux of $(2.3\pm 0.57)\times 10^{-7}$ photons cm^{-2} s^{-1} for γ -rays with energies ≥ 100 MeV, and a photon spectral index of 2.51 ± 0.36 .

The broad-band X-ray observations in 1984 and 1985 with *EXOSAT* described by Singh et al.(1990), showed that its X-ray spectrum is best fitted by a power-law with photon index $\Gamma=1.40\pm 0.35$ and low energy absorption consistent with the Galactic value of N_{H} in its direction ($8.1\times 10^{20}\text{cm}^{-2}$) as given by Stark et al.(1992). The 2–10 keV flux from *EXOSAT* observations, was found to be 8.9×10^{-12} ergs cm^{-2} s^{-1} in the observer’s frame. The source is highly luminous with its X-ray luminosity alone being $\simeq 7\times 10^{45}$ ergs s^{-1} , assuming isotropic emission, redshift of 0.361, $H_o = 50$ km s^{-1} Mpc^{-1} , and $q_o = 0$ in the Friedmann cosmology.

In this letter, we present new *ASCA* observations of PKS 1510-089, along with an analysis of archival *ROSAT* data. Details of the observations and data reduction are given in §2, and the results from the spectral analysis in §3. We discuss our findings in §4.

2. OBSERVATIONS AND DATA REDUCTION

2.1. *ASCA*

PKS 1510-089 was observed with *ASCA* on 1996 August 20 as part of the guest observer program (see Table 1 for the log of observations). The *ASCA* observatory (Tanaka

et al.1994), contains four imaging thin-foil grazing incidence X-ray telescopes, two of which are equipped with Solid State Imaging Spectrometers (SIS) and the other two with Gas Imaging Spectrometers (GIS). SIS detectors have been described in detail by Burke et al. (1991), and GIS by Ohashi et al. (1996) and Makishima et al. (1996). Their properties have been summarized, e.g., in Singh et al. (1996). Due to radiation damage since the launch of ASCA, at the time of the observations reported here the spectral resolution of the SIS detectors had been degraded to $\sim 10\%$ at 1 keV. This spectral resolution is taken into account by the response matrix generated as part of the analysis of this spectrum.

The data were selected as described in Singh et al. (1996) using the FTOOLS/XSELECT software package. PKS 1510-089 is the only source detected in the field of view. The counts and pulse height spectra were accumulated from a source region of 4 arcmin radius in the SIS and 6 arcmin radius in the GIS, while the background was taken from the off-axis source-free regions in the SIS and GIS where counts from the outer wings of the point spread function of the source were minimized. The source spectra were grouped to have a minimum of 20 counts per energy channel prior to spectral analysis (see §3). We have compared our results to those obtained assuming background spectra accumulated from deep observations of blank sky, and obtain consistent results (within statistical uncertainties).

Steady X-ray emission from PKS 1510-089 was detected with a count rates of ~ 0.18 and ~ 0.14 counts s^{-1} above background in SIS0 and SIS1 detectors and in energy bands of 0.5 – 8.2 keV and 0.65 – 8.0 keV respectively. Similarly, the count rates observed with GIS2 and GIS3 were ~ 0.12 and ~ 0.14 counts s^{-1} in the energy bands of 0.75 – 9.7 keV and 0.70 – 10.0 keV respectively. No significant variability was seen on time scales of minutes to hours in any of the detectors. The average X-ray flux in the 0.4 – 10 keV energy band in the observer’s frame was $\sim 1.1 \times 10^{-11}$ ergs $cm^{-2} s^{-1}$ which implies an X-ray luminosity

of $\sim 10^{46}$ ergs s^{-1} ($z=0.361$; $H_o = 50$ km s^{-1} Mpc $^{-1}$; $q_o = 0$ in the Friedmann cosmology). Similarly, the 2–10 keV flux in the observer’s frame, was 8.6×10^{-12} ergs cm^{-2} s^{-1} which is within 4% of the value observed with EXOSAT, consistent with the uncertainties in the cross-calibration of the absolute fluxes of the two satellites. The flux estimates are based on the best fit spectral models described in §3.

2.2. *ROSAT*

PKS 1510-089 was detected in the *ROSAT* all sky survey (RASS) as well as during the pointed observations (Siebert et al. 1995). We have retrieved the publicly-available *ROSAT* data from the pointed observations from the archives maintained at NASA High-Energy Astrophysics Science Archive Research Center (HEASARC). The pointed observations were carried out on 1992 August 17 as part of the *ROSAT* Guest Observer Program, utilizing a position sensitive proportional counter (PSPC) as the focal plane detector (Trümper 1983; Pfeffermann et al. 1987). The PSPC has a field of view of 2° , an energy resolution (FWHM) of 0.42% at 1 keV and a nominal (gain-sensitive) bandwidth for $>10\%$ efficiency of 0.1–2.0 keV. No other X-ray source was detected in the neighborhood of PKS 1510-089. The details of the observations are given in Table 1. The on-source counts were selected from a circular region having a radius of about 3.25 arcmin and centered on the source. An X-ray spectrum from the region was accumulated for the entire observation. The background was accumulated from several neighboring regions at approximately the same offset as the source. The spectral data from the source were binned from the original 256 channels by grouping the first 176 channels by 8 and the rest by 16 to improve the signal-to-noise ratio in each energy bin. These observations resulted in a reasonably good quality spectra with typical signal-to-noise ratio per bin of 5σ .

Steady soft X-ray emission from PKS 1510-089 was detected with a count rate of ~ 0.18

counts s^{-1} above background in the energy range of 0.13 – 2.0 keV in the observer’s frame. According to Siebert et al.(1995), the source flux changed by a factor of ~ 3.5 between the RASS and the pointed mode observation about 2 years later. The average X-ray flux in the 1992 pointed mode observation in the 0.1 – 2 keV energy band was 2.1×10^{-12} ergs cm^{-2} s^{-1} in the observer’s frame. The flux estimate is based on the best fit spectral models in §3.

3. SPECTRAL ANALYSIS AND RESULTS

3.1. ASCA

We have analyzed the X-ray spectra obtained from SIS data for $E \geq 0.5$ keV and the GIS data for energies ≥ 0.7 keV. The spectra were analyzed using XSPEC v9.0 (Arnaud 1996). We first analyzed the data from each detector separately using a simple absorbed power-law model with absorption cross-sections and abundances from Morrison & McCammon (1983). The spectra SIS0, SIS1, GIS2 and GIS3 all gave consistent results. The analysis was then performed jointly on the 2 SIS detectors, and on the 2 GIS detectors; and finally on all the four detectors jointly. We fit the spectra from all four instruments simultaneously, but allowing the normalization of the model to be free for each detector to account for differences in the absolute flux calibrations of the instruments. The results based on the joint analyses of all 4 detectors are given in Table 2. The results are consistent with the analysis of spectra from individual detectors, analyzed separately. The observed spectra from the 4 detectors along with the best fit model of an absorbed power-law are shown separately for SIS detectors in Figure 1, and for GIS detectors in Figure 2. The fit is very good, having a reduced chi-square statistic, $\chi^2_\nu = 1.03$. The resulting spectrum is hard with a photon index $\Gamma = 1.30^{+0.06}_{-0.06}$ (where the errors are at 90% confidence for one parameter of interest), and an equivalent hydrogen column density estimated from low-energy absorption of $N_H = 16 \pm 4 \times 10^{20}$ cm^{-2} which is about twice that due to absorption in our galaxy (see

§1). The same result is obtained if assume an absorber at $z=0.361$, along with a fixed absorption from 21-cm measurements in our galaxy. In Figure 3 we show the 68%, 90%, and 99% confidence contours for the values of the spectral index and the N_{H} allowed by the data. Motivated by an earlier report about the presence of a Gaussian feature near 5 keV in the spectrum (Singh et al. 1990), we also tried adding a similar feature to the *ASCA* spectra and got a marginal improvement in the quality of the fit. The best fit line position was at 5.1 ± 0.4 keV with an equivalent width of about 87 eV. Considering the signal to noise in this portion of the spectrum and the fact that the overall fit improved only marginally, we regard this equivalent width as an upper limit. The equivalent width of the emission line suggested by an *EXOSAT* observation (Singh et al 1990) was several times higher, suggesting that either the line varied or it was spurious. Alternate models e.g., (i) a broken power-law with a low-energy index Γ_l , a break at energy $E_c \sim 0.9$ keV, and a high-energy index Γ_h , or (ii) the addition of a blackbody to a simple power-law, or (iii) a partially covered power-law, provided equally good fits to the spectra (see Table 2). The improvement in the fit was insignificant, however. Therefore, the data are not able to distinguish between the absence or the presence of a low-energy excess in the spectrum.

3.2. *ROSAT*

Results from our spectral analysis of the *ROSAT* PSPC data are presented in Table 3. A simple absorbed power-law model provided a good fit to the PSPC spectrum. The data and our best fit power-law model are shown in Figure 4. The confidence contours for the spectral index and the hydrogen column density N_{H} allowed by the PSPC data are shown in Fig. 3. The best fit spectral index, $\Gamma=1.88\pm 0.28$ is significantly higher than that measured during the *ASCA* observations. The corresponding column density N_{H} , is $(7.6^{+2.0}_{-1.5})\times 10^{20}$ cm^{-2} , which is consistent with the 21-cm value. The unabsorbed flux at 1

keV is $\sim 10\%$ lower than in the *ASCA* observations. The apparent discrepancy between the *ROSAT* and *ASCA* observations imply that either variations in both the spectral index and the absorbing column occurred between the two epochs, or that the PSPC band is dominated by a separate, steep spectral component. The PSPC spectra could be fit equally well by a broken power-law ($\Gamma_l = 1.9 \pm 0.2$, with the hard component fixed at $\Gamma_h = 1.30$) with absorption, however the break energy cannot be constrained (see Table 3.). A model consisting of a low-energy blackbody and hard power-law also provides a statistically acceptable description of the data. However, such a model requires a value of N_H less than the Galactic value and hence we consider it unrealistic. The PSPC data show no preference for any of the three models.

3.3. *ROSAT* and *ASCA* Combined Spectral Analysis

If we accept the simple absorbed power-law then there is a significant difference between the spectral index and N_H observed by *ROSAT* in 1992 compared to that observed by *ASCA* 4 years later. Since there were no measurements above 2 keV in 1992, the hard X-ray flux seen with *ASCA* might have varied even though the 1-keV flux hardly changed. In that case, joint fitting of *ROSAT* and *ASCA* data would not be meaningful. In the likely case that a more complex spectrum is present with a change around 1-keV, the joint fitting can constrain the additional parameters involved in multi-component models. We, therefore, carried out multi-component, multi-instrument model fitting, the results of which are given in Table 4. We fit the spectra from all five instruments simultaneously, but allowing the normalization of the model to be free for each detector to account for differences in the absolute flux calibrations of the instruments and changes in source intensity between the two epochs. As expected, a simple power-law model gives an acceptable fit only if the N_H is allowed to be significantly lower than the Galactic value in the direction of PKS 1510-089.

Both the broken power-law and blackbody plus power-law models give acceptable fits to the data with the N_{H} value almost consistent with the Galactic value (see Table 4). A partially covered power-law model with Galactic absorption and a very high absorption intrinsic to the source at $z=0.361$, gives a somewhat poorer fit. Thus we conclude that the most likely explanation of the *ROSAT* & *ASCA* observations is that a powerlaw of photon index $\Gamma \simeq 1.3$ dominates the spectrum above $\gtrsim 1$ keV with a 2–10 keV flux $\simeq 8.6 \times 10^{-12}$ ergs cm^{-2} s^{-1} at both epochs in the observer’s frame. A separate, steeper spectral component dominates at lower energies, the specific form of which cannot be unambiguously determined.

4. DISCUSSION

ASCA observations show that the 0.5 – 10 keV X-ray spectrum of PKS 1510-089 is hard ($\Gamma \simeq 1.3$). Although earlier observations with the *EXOSAT* (Singh et al.1990; Sambruna et al.1994) had indicated that the X-ray spectrum of PKS 1510-089 might be this hard, those measurements were not conclusive due to a relatively poor signal-to-noise ratio. The observed spectral index is significantly flatter than that of the typical radio-loud quasars ($\langle \Gamma \rangle = 1.66 \pm 0.07$, Lawson et al.1992; Cappi et al.1997), radio-quiet quasars ($\langle \Gamma \rangle = 1.90 \pm 0.11$, Lawson et al.1992; Williams et al.1992), and BL Lac objects ($\langle \Gamma \rangle = 2.20_{-0.15}^{+0.17}$, Sambruna et al.1994). The observed spectrum is, however, similar to that of other HPQs observed in both the hard (e.g. 3C 345 with $\Gamma = 1.4 \pm 0.09$, Makino 1989; PKS 0537-441 with $\Gamma = 1.26_{-0.31}^{+0.24}$ Sambruna et al. 1994) and the soft (e.g. 0212+735 with $\Gamma = 0.44_{-0.41}^{+0.39}$ and 0836+710 with $\Gamma = 1.4 \pm 0.05$, Brunner et al.1994) X-ray bands. Thus, based on an admittedly small number of examples, HPQs do appear to show X-ray spectra that are flatter than those of other core-dominated radio-loud quasars.

PKS 1510-089 was observed in the near ultraviolet band with the International Ultraviolet Explorer (IUE) low-dispersion spectrographs during the early 1980s. There

are three SWP exposures and two LWR exposures in the archive. The SWPs include one nondetection and two spectra obtained over a nominal 1-year baseline whose continuum levels are equivalent to the 1σ level. One LWR exposure was underexposed and resulted in a nondetection. There is, however, no evidence of variability in the available UV data, although it cannot be ruled out either. Though weakly detected on one occasion with the short- and long- wavelength instruments, redshifted emission lines of Ly- α and O VI/Lyman- β are clearly detected, with several other normally prominent emission lines possibly present. The UV continuum is well approximated by a power law with index -1.2 (ν vs f_ν).

We constructed a multifrequency spectrum using measurements from the published literature. The spectrum is shown in Figure 5. We note that these data do not result from simultaneous or even contemporaneous observations. The “radio” points at 1.5 and 4.9 GHz are from O’Dea et al. (1985); we note however that Aller et al. (1996), who present a 20-year radio light curve for PKS 1510-089, show that it varies by at least factors of 5, mainly in series of flare-like events occurring on yearly time scales (and sometimes persisting for months). The near IR measurement at $1.5\mu\text{m}$ is from Landau et al. (1986) and we used the visual magnitude of $V=16.5$ of Bolton & Elkers (1966) to derive a flux point corresponding to 5500 \AA . We used the UV measurements obtained from the IUE archives as described previously. The optical and UV fluxes have been corrected for galactic extinction using the extinction law of Seaton (1979) and a color excess estimated from the galactic N_{H} values derived from the 21-cm measurements. The γ -ray flux at energies ≥ 100 MeV has been taken from *EGRET* measurements (Thompson et al 1993).

The multiwaveband spectrum of PKS 1510-089 resembles that of many other blazars detected by *EGRET*, with the bulk of the luminosity being emitted as γ -rays (e.g. see Fig.5 of von Montigny et al (1995) – indeed, we note the multiwaveband spectrum of

PKS 1510-089 is globally very similar to the BL Lac Mrk 421). In the popular relativistic jet models, the hard X- and γ -ray emission is proposed to arise as a result of inverse-Compton scattering of low energy photons by relativistic electrons within the jet (e.g., see von Montigny et al (1995), and references therein). We suggest that the double powerlaw form found above might indicate that the *ROSAT* data are dominated by the steep tail of this low energy emission (often assumed to be synchrotron radiation) while the flatter inverse-Compton scattered component dominates the *ASCA* data > 1 keV. We suggest that even though superluminal motion has not (yet) been detected in this source, the emission is likely to be relativistically beamed.

Based on Figure 5, PKS 1510-089 may be among a subclass of blazar AGN which exhibit the so called big blue-bump component. In order to study the blue-bump emission, we subtracted a power-law component, connecting the X-ray, IR, and mm radio points, from the multifrequency spectrum to obtain residuals in the optical-UV region. A statistically significant, positive residual is obtained. We emphasize that variability could account for some or all of this apparent residual. We then fit a thermal accretion disk spectrum to these residual spectra. The model involves thermal emission due to viscous dissipation in a steady-state, accretion disk which has been modified to include the effects of gravitational red-shift and focusing (e.g. Sun & Malkan, 1989); we have employed computational methods similar to those described in Czerny et al. (1986). A Schwarzschild metric was used in the calculations and an inclination of $\sin i = 0.5$ was assumed. We fixed the inner disk radius at $3R_g$ and $R_{out}/R_{in} \simeq 200$. We were unable to obtain a reasonable fit to the optical and UV data without reducing R_{out}/R_{in} to this level; values more typically fitted to AGN are of order $R_{out}/R_{in} \simeq 10^3$. Again, this could possibly be attributed to variability – we suspect that the actual visual flux at the time of the UV measurements may have been significantly higher.

If the blue-bump residual we depict here is NOT an artifact of non-simultaneous measurements of a highly variable source, PKS 1510-089 is among a minority of the extreme blazar AGN which both emit gamma-rays and exhibit a blue-bump component. Another blazar with a blue-bump component is 3C 345 (e.g. Webb et al 1994), but it was never detected at more than a 3.5σ level with *EGRET*.

A detailed discussion of the various physical models proposed for such objects is beyond the scope of the current paper. Further simultaneous, broad-band UV, X- & γ -ray observations are required to constrain physical models.

We wish to thank the entire *ASCA* team for making these observations possible. This research has made use of *ROSAT* archival data obtained through the High Energy Astrophysics Science Archive Research Center, HEASARC, Online Service, provided by the NASA-Goddard Space Flight Center.

REFERENCES

- Aller, H.D., Aller, M.F. & Hodge, P.E. 1981, AJ, 86, 325
- Aller, M.F., Aller, H.D., & Hughes, P.A., 1996, in Proceedings of “Blazar Continuum Variability”, ASP CS-110, p193.
- Anders, E., & Grevesse, N., 1989, *Geochimica et Cosmochimica Acta*, 53, 197
- Arnaud, K.A., 1996, *Astronomical Data Analysis Software and Systems V* eds Jacoby, G., Barnes, J, p17, ASP Conf. Series vol 101.
- Appenzeller, I. & Hiltner, W. A. 1967, ApJ, 149, L17
- Bolton, J.G. & Ekers, J. 1966, *Austr. J. Phys.*, 19, 559
- Brunner, H., Lamer, G., Worrall, D.M. & Staubert, R., 1994, *A & A*, 287, 436
- Burbidge, E.M. & Kinman, T.D. 1966, ApJ, 145, 654
- Burke, B.E., Mountain, R.W., Harrison, D.C. et al., 1991, *IEEE Trans.*, ED-38, 1069
- Cappi, M., Matsuoka, M., Comastri, A., Brinkmann, W., Elvis, M., Palumbo, G.C.C., & Vignali, C., 1997, ApJ, 478, 000
- Czerny, B., Czerny, M., & Grindlay, J.E., 1986, ApJ, 311, 241
- Eraclous, M., Halpern, J.P., & Livio, M. 1996, ApJ, 459, 89
- George, I.M., Nandra, K., Turner, T.J. & Celotti, A. 1994, ApJ, 436, L59.
- Landau, R. et al.1986, ApJ, 308, 78
- Lawson, A.J., Turner, M.J.L., Williams, O.R., Stewart, G.C., & Saxton, R.D., 1992, 259, 743

- Liller, M.H. & Liller, W. 1975, ApJ, 199, L133
- Lu, P. K. 1972, AJ, 77, 829
- Makino, F. in Proc. of 23rd ESLAB Symp., ESA publications SP-296, volume 2, p803
- Makishima, K. et al. 1996, PASJ, 48, 171
- Malkan, M.A. & Moore, R.L. 1986, ApJ, 300, 216
- Morrison, R. & McCammon, D. 1983, ApJ, 270, 119
- O’Dea, C.P., Barvainis, R. & Challis, P.M. 1988, AJ, 96, 435
- Ohashi, T. et al. 1996, PASJ, 48, 157.
- Pfeffermann, E., et al. 1987, Proc. SPIE Int. Soc. Opt. Eng., 733, 519
- Sambruna, R.M., Barr, P., Giommi, P., Maraschi, L., Tagliaferri, & Treves, A., 1994, ApJ, 434, 468.
- Seaton, M.J., 1979, MNRAS, 187, 73
- Siebert, J., Brinkmann, W., Marganti, R., Tadhunter, C.N., Danziger, I.J., Fosbury, R.A.E., & S. di Serego Aligheri, 1995, MNRAS, 279, 1331.
- Singh, K.P., Rao, A.R., and Vahia, M.N. 1990, ApJ, 365, 455
- Singh, K.P., White, N.E., & Drake, S.A., 1996, ApJ, 456, 766
- Sreekumar, P. et al.1996, ApJ, 464, 628
- Stark, A.A., Gammie, C.F., Wilson, R.W., Bally, J., Linke, R.A., Heiles, C., & Hurwitz, M., 1992, ApJS, 79, 77.
- Steppe, H. et al.1988, A & AS, 75, 317

Sun, Wei-Hsin & Malkan, M.A., 1989, ApJ, 346, 68

Tanaka, Y., et al., 1994, PASJ, 46, L37

Thompson, D.J., et al., 1993, ApJ, 415, L13

Trüemper, J. 1983, Adv. Space Res., 2, 241

Turner, T.J., George, I.M., Madejski, G.M., Kitamoto, S., & Suzuki, T., 1995, ApJ, 445,

von Montigny et al., 1995, ApJ, 440, 525

Webb, J.R. et al., 1994, ApJ, 422, 570

Williams, O.R., et al., 1992, ApJ, 389, 157

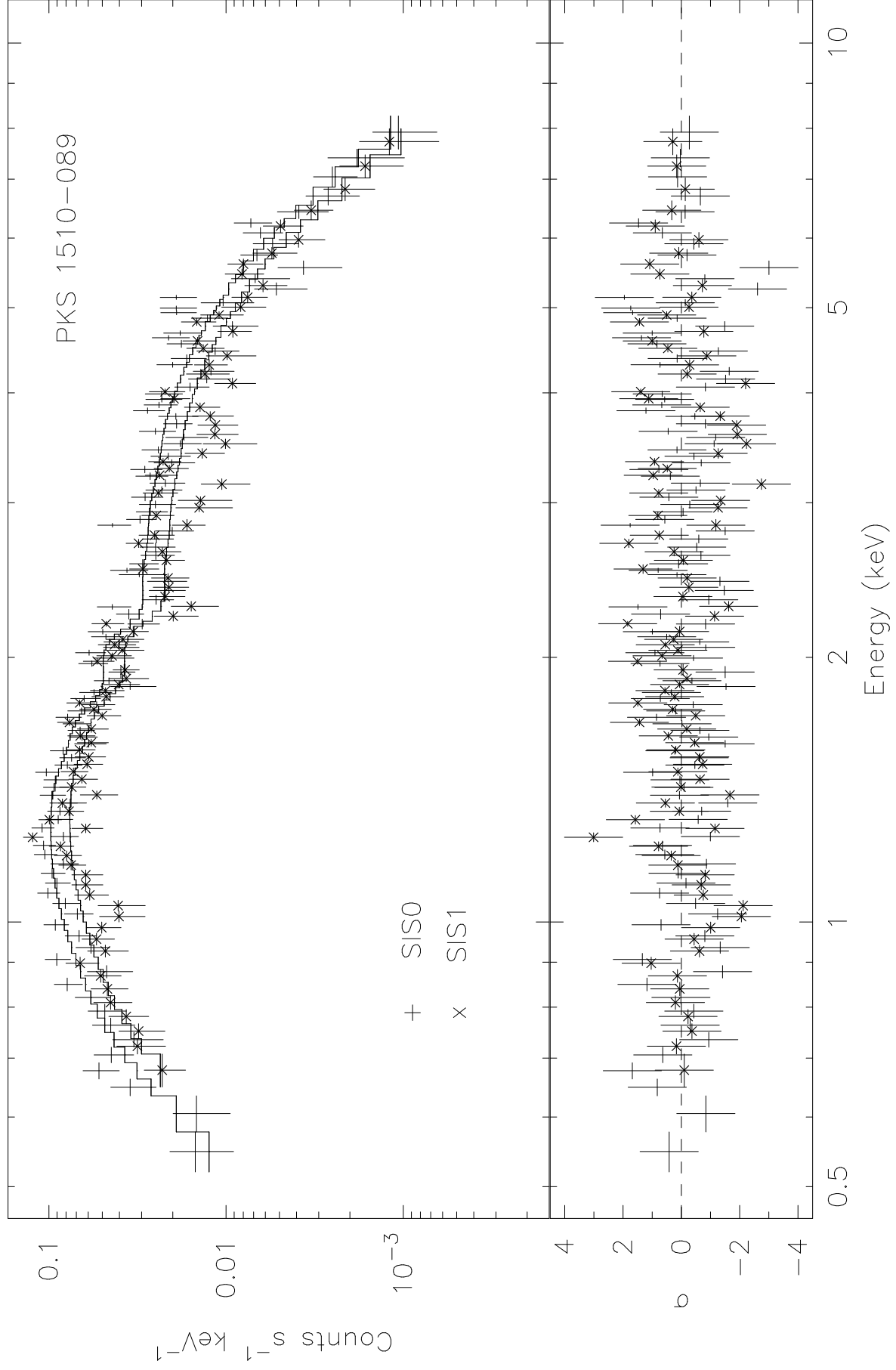
Fig. 1.— Best-fit SIS spectra from a joint fit to the SIS and GIS spectra are shown after fitting with a single absorbed power-law (upper panel). The best fit model is shown as a histogram. The departures from the best fit are shown in the lower-panel as the number of σ s with an error bar of 1σ .

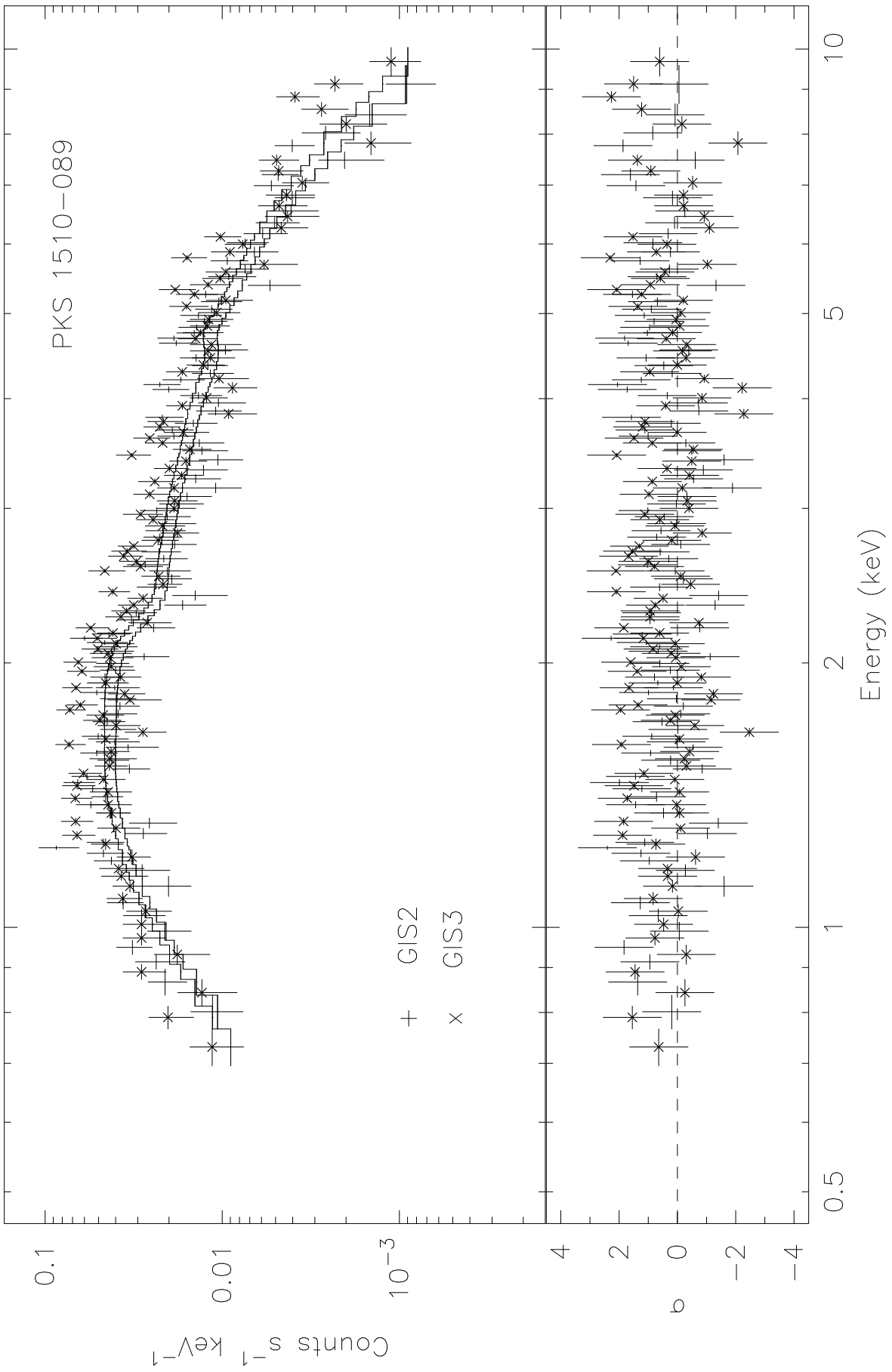
Fig. 2.— Same as in Figure 1, but for the GIS spectra.

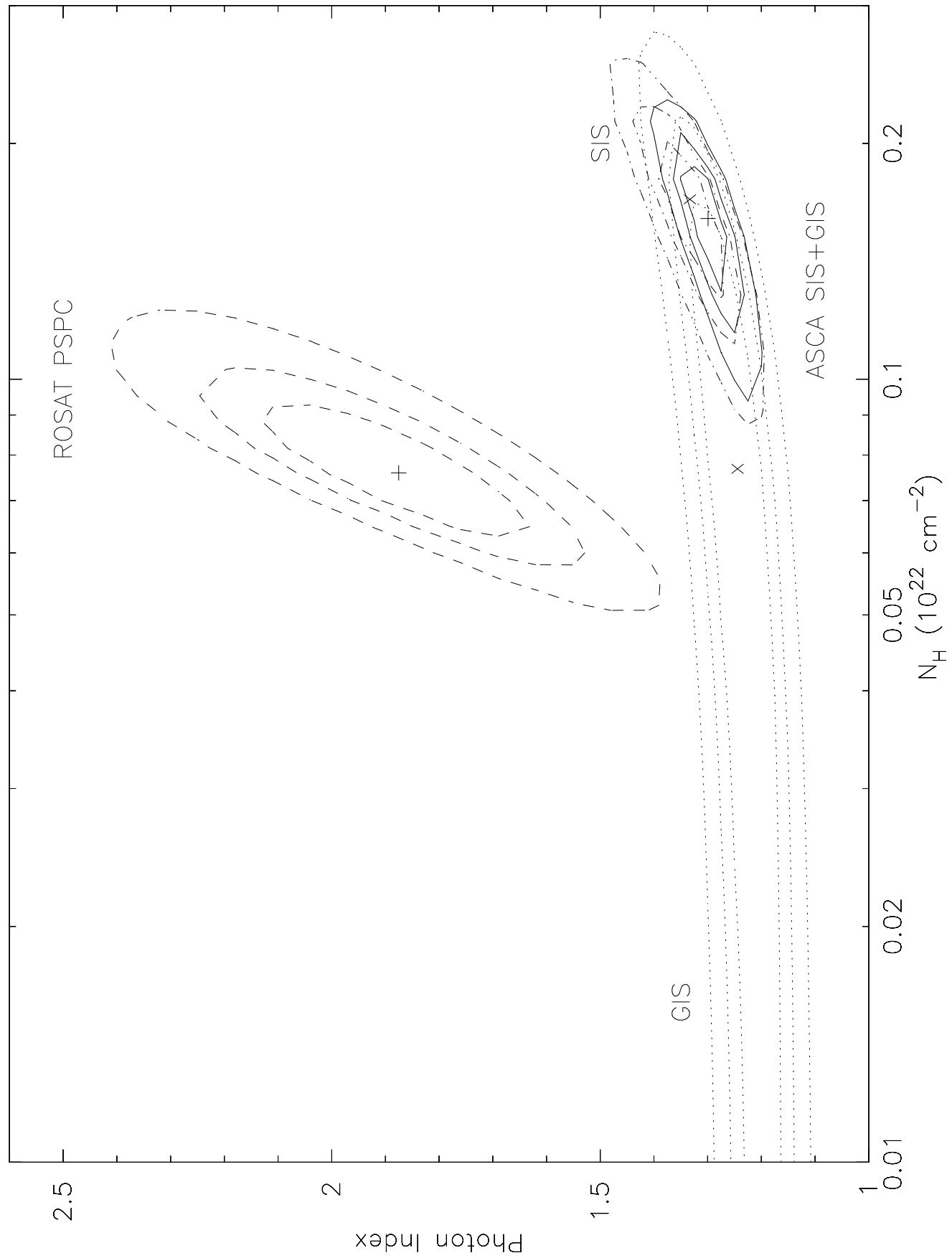
Fig. 3.— Allowed ranges of the N_H and Γ from the X-ray spectrum of PKS 1510-089 based on the χ^2 contours. The full contours represent the 68%, 90%, and 99% confidence limits from fitting SIS+GIS together, the dashed-dotted contours show similar confidence levels for the SIS data alone, the dotted contours for the GIS data alone, and the dashed contours are for the PSPC data alone. The plus, cross, cross, and plus mark the best fit values.

Fig. 4.— Best-fit PSPC spectra using a single absorbed power-law, shown in the same way as for the Figs. 1 and 2.

Fig. 5.— Broadband spectral energy distribution of PKS 1510–089 based on the (non-contemporaneous) multifrequency measurements cited in the text. The dotted line represents a powerlaw fit to the mm, IR and X-ray measurements, with a superposed multi-color blackbody disk fit to the apparent blue-bump residual. The outer disk radius required to obtain the fit was much smaller than is normally the case for radio quiet AGN – we suspect that the actual optical flux at the time of the UV measurements was probably higher.







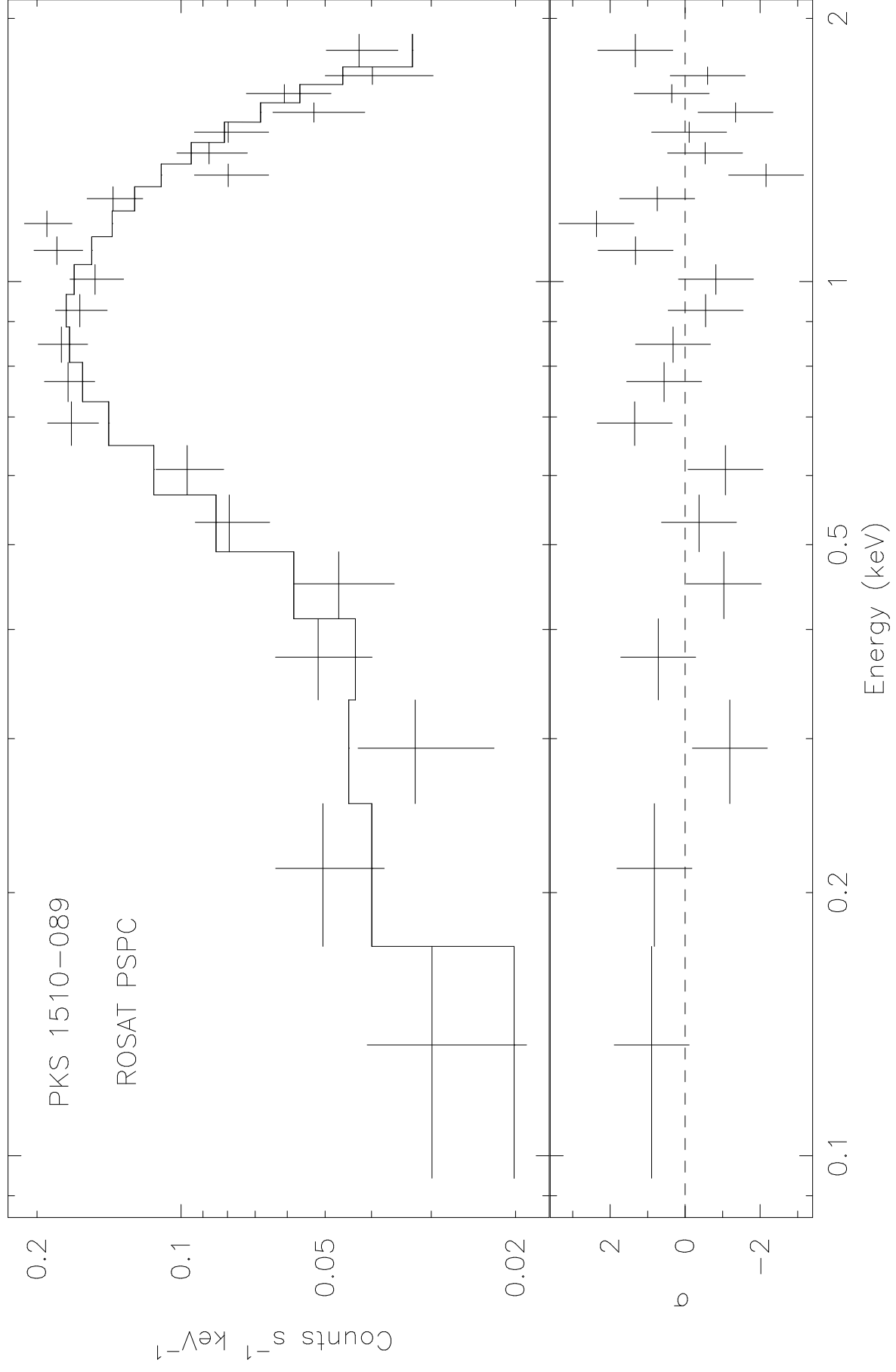


TABLE 1
OBSERVATION LOG FOR PKS 1510-089

Satellite Name	Detector Name	Date	Exposure (seconds)	Count Rate ^a (Counts s ⁻¹)	Energy Range ^b (keV)
ROSAT	PSPC	1992 Aug 17	5153	0.176±0.006	0.13 – 1.9
ASCA	SIS0	1996 Aug 20	18317	0.180±0.004	0.51 – 8.2
ASCA	SIS1	1996 Aug 20	18105	0.141±0.003	0.65 – 8.0
ASCA	GIS2	1996 Aug 20	18301	0.118±0.003	0.75 – 9.7
ASCA	GIS3	1996 Aug 20	18300	0.138±0.003	0.70 – 10.0

^aAfter background subtraction.

^bIn observer frame.

TABLE 2
RESULTS FROM ANALYSIS OF SIS & GIS SPECTRA

Model	N _H 10 ²⁰ cm ⁻²	Γ _h	A ^a	Γ _l or kT _{bb} ^b or pcf ^c	E _{bk} ^d or L _{bb} ^d	χ ² /dof	E _l keV	EW eV
Power-law	16.0 ^{+4.0} _{-3.7}	1.30 ^{+0.06} _{-0.06}	11.2	–	–	458.3/444	–	–
Power-law +Gaussian	16.6 ^{+3.4} _{-3.6}	1.32 ^{+0.03} _{-0.05}	11.4	–	–	453.5/442	5.1±0.5	87
Broken Power-law	17.2 ^{+6.1} _{-4.8}	1.31 ^{+0.07} _{-0.06}	10.8	1.8 ^{+1.1} _{-1.4}	0.9	458.1/442	–	–
Broken Power-law +Gaussian	18.0 ^{+5.0} _{-3.0}	1.33 ^{+0.06} _{-0.05}	11.7	1.8 ^{+1.3} _{-1.3}	0.9	453.1/440	5.1±0.5	88
Power-law +Blackbody	11.3 ^{+5.0} _{-3.5}	1.07 ^{+0.17} _{-0.10}	7.6	0.45	<1.0	452.2/442	–	–
Partially covered Power-law ^e	32 ⁺⁸⁰ ₋₂₅	1.31 ^{+0.08} _{-0.07}	11.3	0.54 ^{+0.46} _{-0.31}	–	458.4/443	–	–

^aUnabsorbed flux at 1 keV (observer frame) in units of 10⁻⁴ photons cm⁻² s⁻¹ keV⁻¹.

^bΓ₂: Low-energy photon index; kT_{bb}: Blackbody temperature in keV.

^cpcf: partially covering fraction of the source.

^dE_{bk}: Break energy in keV for the broken power-law; L_{bb}: Total Blackbody luminosity in 10⁴⁴ergs s⁻¹.

^eFixed N_H = 8.1 × 10²⁰ cm⁻² due to galaxy + absorption at z = 0.361.

Notes: Errors and upper limits are with 90% confidence based on χ²_{min}+2.71

TABLE 3
RESULTS FROM ANALYSIS OF PSPC SPECTRUM

S.	Model	N_H	Γ_h	A^a	Γ_l	E_{bk}^c	χ^2 /dof	F_{SX}^d	L_{SX}^e
No.		10^{20} cm^{-2}			or kT_{bb}^b	or L_{bb}^c			
1.	Power-law	$7.6^{+2.0}_{-1.5}$	1.88 ± 0.28	10.2	–	–	25.9/20	2.1	3.5
2.	Broken Power-law	$7.7^{+2.0}_{-1.7}$	1.30	10.2	1.9 ± 0.2	$1.6^{+inf}_{-0.4}$	25.6/19	2.1	3.6
3.	Power-law +Blackbody	$5.1^{+1.5}_{-1.3}$	1.30	6.2	0.21 ± 0.05	7.0 ± 4.0	24/18	2.0	2.2

^aUnabsorbed flux at 1 keV (observer frame) in units of $10^{-4} \text{ photons cm}^{-2} \text{ s}^{-1} \text{ keV}^{-1}$.

^b Γ_2 : Low-energy photon index; kT_{bb} : Blackbody temperature in keV.

^c E_{bk} : Break energy in keV for the broken power-law; L_{bb} : Total Blackbody luminosity in $10^{44} \text{ ergs s}^{-1}$.

^dAbsorbed flux between 0.1 – 2.0 keV (observer frame) in units of $10^{-12} \text{ ergs cm}^{-2} \text{ s}^{-1}$.

^eIntrinsic Luminosity (no absorption) between 0.1 – 2.0 keV (observer frame) in units of $10^{45} \text{ ergs s}^{-1}$.

Notes: Errors and upper limits are with 90% confidence based on $\chi^2_{\text{min}} + 2.71$

TABLE 4
RESULTS FROM JOINT ANALYSIS OF PSPC, SIS & GIS SPECTRA

Model	N_H	Γ_h	A^a	Γ_l	E_{bk}^d	χ^2 /dof
	10^{20} cm^{-2}			or kT_{bb}^b	or L_{bb}^d	
				or pcf ^c		
Power-law	$5.1^{+1.1}_{-0.7}$	$1.17^{+0.04}_{-0.03}$	9.3	–	–	531.2/466
Broken Power-law	$11.3^{+3.0}_{-3.0}$	$1.24^{+0.04}_{-0.04}$	4.9	$3.5^{+0.0}_{-1.2}$	$0.70^{+0.10}_{-0.10}$	520.7/464
Power-law +Blackbody	$11.8^{+2.0}_{-1.6}$	$1.25^{+0.05}_{-0.05}$	10.4	$0.056^{+0.01}_{-0.01}$	7.6	520.3/464
Partially covered Power-law ^e	200^{+220}_{-50}	$1.30^{+0.17}_{-0.05}$	11.3	$0.15^{+0.75}_{-0.12}$	–	538.1/465

^aUnabsorbed flux at 1 keV (observer frame) in units of $10^{-4} \text{ photons cm}^{-2} \text{ s}^{-1} \text{ keV}^{-1}$.

^b Γ_2 : Low-energy photon index; kT_{bb} : Blackbody temperature in keV.

^cpcf: partially covering fraction of the source.

^d E_{bk} : Break energy in keV for the broken power-law; L_{bb} : Total Blackbody luminosity in $10^{45} \text{ ergs s}^{-1}$.

^eFixed $N_H = 8.1 \times 10^{20} \text{ cm}^{-2}$ due to galaxy + absorption at $z = 0.361$.

Notes: Errors and upper limits are with 90% confidence based on $\chi^2_{\text{min}} + 2.71$

PKS 1510-089

